Vol 18 No 9, September 2009
1674-1056/2009/18(09)/4007-06

Chinese Physics B

© 2009 Chin. Phys. Soc.
and IOP Publishing Ltd

Structural, electrical and optical characterization of InGaN layers grown by MOVPE*

Yıldız A[a], Öztürk M Kemal[b]†, Bosi M[c], Özçelik S[d], and Kasap M[d]

[a] *Physics Department, University of Ahi Evran, Asikpasa Kampusu,* 40040, *Kirsehir, Turkey*
[b] *Mineral Analysis and Technology Department, MTA,* 06520 *Ankara - Turkey*
[c] *IMEM-CNR Institute, Area delle Scienze 37/A, I-*43010 *Fontanini, Parma, Italy*
[d] *Physics Department, University of Gazi,* 06500 *Teknikokullar, Ankara, Turkey*

(Received 11 February 2008; revised manuscript received 24 August 2008)

We present a study on n-type ternary InGaN layers grown by atmospheric pressure metalorganic vapour phase epitaxy (MOVPE) on GaN template/(0001) sapphire substrate. An investigation of the different growth conditions on n-type $In_xGa_{1-x}N$ ($x = 0.06 - 0.135$) alloys was done for a series of five samples. The structural, electrical and optical properties were characterized by high resolution x-ray diffraction (HRXRD), Hall effect and photoluminescence (PL). Experimental results showed that different growth conditions, namely substrate rotation (SR) and change of total H_2 flow (THF), strongly affect the properties of InGaN layers. This case can be clearly observed from the analytical results. When the SR speed decreased, the HRXRD scan peak of the samples shifted along a higher angle. Therefore, increasing the SR speed changed important structural properties of InGaN alloys such as peak broadening, values of strain, lattice parameters and defects including tilt, twist and dislocation density. From PL results it is observed that the growth conditions can be changed to control the emission wavelength and it is possible to shift the emission wavelength towards the green. Hall effect measurement has shown that the resistivity of the samples changes dramatically when THF changes.

Keywords: InGaN, MOVPE, substrate rotation, total H_2 flow
PACC: 7470H, 7855, 7340H, 7870C

1. Introduction

In recent years, nitride semiconductors have been widely used in opto-electronic and micro-electronic device fabrication.[1,2] Group-III nitrides, InN, GaN and AlN, form the active layers for (Al, In) GaN-based light emitting diodes (LEDs) and laser diodes (LDs) whose emission wavelength ranges from green to ultraviolet light. Due to their wide band gap, InGaN alloys are the basis for the fabrication of green–blue LEDs, either with a simple p/n junction or with quantum well structures. The larger the In molar fraction is, the smaller the bandgap. The emission shifts from ultraviolet in the case of very low In content (< 0.03) to green when the In fraction is larger (> 0.2). Several growth parameters affect the final In/Ga ratio in the epilayers.[3−5] Therefore, in this study the In fraction in the crystal, determined by high resolution x-ray diffraction (HRXRD), is varied by imposing different growth parameters. Namely, we examined samples grown under different total H_2 flow (THF) and substrate rotation (SR). Little work exists on the effect of these parameters on the electrical and structural properties.

Allowing small amounts of hydrogen to flow in the growth chamber has a profound effect on the InN percent in InGaN epitaxial films.[6] The driving force for the deposition of InN decreases significantly with an increase in hydrogen partial pressure and hydrogen affects the vapour–solid relationship and the formation of the inhomegeneous composition in $In_xGa_{1-x}N$ growth.[6] The addition of hydrogen to nitrogen during the growth of GaN by MOCVD results in changes in the gas flow pattern and decreases the growth rate.[7,8] A higher SR speed leads to higher growth rate and, consequently to a higher In molar fraction incorporated in the layer. Therefore the SR has a remarkable influence on the growth rate of the $In_xGa_{1-x}N$ layer. This is a well-known flow-dynamic effect which finally improves the mass transport from the gas phase (basically the rotating substrate acts as a fan which sucks the fluid axially and expels it tangentially).[4,9]

The aim of the present work is to investigate the

*Project supported by the State Planning Organization of Turkey (Grant No 2001K120590).
†Corresponding author. E-mail: ozturkm@gazi.edu.tr

effect of different growth conditions on the properties of InGaN/GaN heterostructures with HRXRD, PL and the Hall effect. Pseudomorphically strained $In_xGa_{1-x}N$ layers, grown by MOVPE on GaN with different SR and THF conditions, were analysed by HRXRD scans in order to assess the layer crystalline quality, In composition and strain. Defects in the buffer layers including tilt, twist and dislocation density were investigated and prensented as a function of SR. The electrical properties of $In_xGa_{1-x}N$ alloys were investigated by Hall effect measurements both at room and low temperatures. Finally, the results of PL investigation at room temperature are presented and discussed.

2. Experimental

InGaN epilayers studied in this work were grown in an atmospheric pressure vertical MOVPE reactor with a 'shower head' configuration. The precursors used were the standard ammonia, Trimethyl Gallium (TMG) and Trimethyl Indium (TMI); N_2 was always taken as the main carrier gas while H_2 was used as the metal-organic carrier. H_2 was also introduced into the reactor in a controlled amount via an additional make-up line: this permitted a degree of control over the indium composition in InGaN layer, since H_2 partial pressure in the growth chamber can control the indium incorporation in the InGaN layer.[4] The TMG precursor was delivered to the reactor via a double dilution source line, which allows changing the Ga molar fraction while maintaining a constant hydrogen flow injection into the growth chamber. The TMI is instead introduced with a standard single dilution line, in which the hydrogen flow enters into a bubbler and the metal-organic is carried to the reactor by a pressure controller. The change in rotation speed is permitted to control the growth rate, which has a strong influence on indium content in the alloy.[10] In this configuration, the hydrogen delivered to the growth chamber is always proportional to the In molar fraction. The 50.8 cm sapphire substrates were rotated around their axis at rates varying between 120 and 750 rpm. The standard heterostructure included a 80–100 nm thick GaN buffer grown at 510 °C, a 600 nm thick GaN layer deposited at 1080 °C (typical V/III ratio was about 7000), and an InGaN alloy deposited at 800 °C with different conditions, as reported above, in order to vary the In content.

The HRXRD measurements were performed by a D8-Discover diffractometer equipped on the primary side with a Ge(220) monochromator. Resistivity and Hall effect measurements were carried out by the van der Pauw method as a function of temperature, using square shaped (5×5 mm^2) samples with four contacts in the corners. Either evaporated or annealed indium dots were deposited on the samples, and their ohmic behaviour was confirmed by the current–voltage characteristics. The measurements were made at different steps over a temperature range 200–350 K using a Lake Shore Hall effect measurement system (HMS). Room temperature photoluminescence was measured using a standard set-up and He–Cd laser excitation operating at 325 nm.

3. Results and discussions

The high resolution close-up view of the diffraction peaks obtained by using HRXRD measurements for four samples with the same THF is shown in Fig.1. The InGaN diffraction peak of the (004) plane is clearly separated from the (004) GaN diffraction peak. The high intensity peaks originate from diffraction of the InGaN buffer layer and other peaks belong to the GaN layers. They show that the positions of InGaN (004) peaks are located approximately near 36°, respectively, with some shift ascribed to the SR speed. The HRXRD shows that the peaks are shifted to higher angles when the SR speed is decreased, as shown clearly in Fig.1. With a different THF value (240 cm^3/min), the peak of sample 128 which has a value of 36.187° for the angle position (not shown here) changes dramatically.

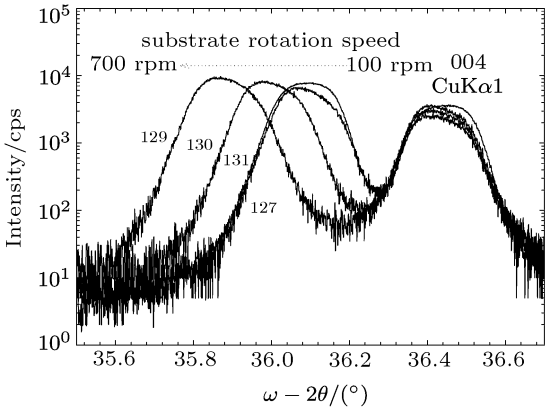


Fig.1. HRXRD scans in the vicinity of the symmetric (004) reflection for samples with the same THF value; high and low intensity peaks belong to InGaN and GaN layers respectively.

In order to investigate the effect of different growth conditions on the crystalline quality and the mosaic structure of the samples, we determined the full width at half maximum (FWHM) values for selected reflections of the samples. The (002), (102) and (121) planes in units of degrees are given in Table 1.

Table 1. The FWHM values (in units of degrees) of (002), (102) and (121) reflection peaks versus SR and THF for InGaN and GaN layers.

sample	rotation /(RPM)	H_2 flow /(cm^3/min)	InGaN (002)	GaN (002)	InGaN (102)	GaN (102)	InGaN (121)	GaN (121)
#128	200	240	0.052	0.047	0.463	0.569	0.523	0.588
#131	100	140	0.075	0.048	0.468	0.489	0.475	0.600
#127	200	140	0.076	0.048	0.359	0.359	0.244	0.244
#130	400	140	0.120	0.074	0.414	0.453	0.614	0.721
#129	675	140	0.145	0.138	0.637	0.749	0.527	0.482

For the (002) reflection planes of InGaN and GaN layers, it was observed that sample 128 with values of 240 cm^3/min THF with 200 rpm SR speed exhibits optimum behaviour.

For samples with the same values of THFs, the FWHM values increase with increasing SR speed. This is only observed in the (002) reflections since the (002) symmetric reflections have higher intensity due to asymmetric planes. When the intensity decreases because of low quality properties, for asymmetric planes this sequence is not observed as shown in Table 1. Moreover, the SR speed does not affect the mosaic structure (i.e. tilt, twist, dislocation density). In the mosaic structure, the calculated tilt and twist values are used for a detailed examination. For tilt computing, a Williamson–Hall plot can be utilized,[11] in which the FWHM of the symmetric rocking curves is a function of the reflection order and FWHM $(\sin\theta)/\lambda$ is plotted against $(\sin\theta)/\lambda$ for each reflection and fitted by a straight line. Here, λ and θ is the x-ray wavelength and the incident angle of the x-rays, respectively. The tilt is then obtained from the slope of the linear dependence. Values of tilt for GaN and InGaN layers are presented in Table 2. The FWHM values of asymmetric (121) reflections give a twist angle that is the out-of-plane rotation of the blocks perpendicular to the surface normal at the larger z-axis angle of the x-ray setup,[12] and twist values for all samples are given in the last column of Table 1. Neither of the properties are affected by the SR speed, and they show increasing or decreasing values, resulting in a stable mosaic structure.

Table 2. The obtained structural parameters of the grown samples.

sample	In content	a/Å	c/Å	$\epsilon_{\|\|} \times 10^{-2}$	$\epsilon_{\mathrm{I}} \times 10^{-2}$	tilt of GaN(InGaN)
#128	0.060	3.211	6.848	–0.668	0.4861	0.461(0.407)
#131	0.095	3.217	6.851	–0.835	0.6067	0.335(0.305)
#127	0.085	3.220	6.853	–0.946	0.6886	0.465(0.425)
#130	0.105	3.227	6.857	–1.168	0.8507	0.327(0.308)
#129	0.135	3.238	6.862	–1.1502	1.0937	0.438(0.356)

The different InGaN peak positions reflect a difference in indium contents for all samples, depending on SR and THF as seen in Fig.1. The determination of lattice parameter and In content by HRXRD is based on a unique relationship between the lattice parameter and the chemical composition which, according to Vegard's rule for semiconductor alloy systems, is generally assumed to be linear.[13,14] The calculated In contents, lattice parameter, the in-plane strain ($\epsilon_{||} = a_{\mathrm{GaN}}/a_{\mathrm{InGaN}} - 1$) and the perpendicular strain ($\epsilon_{\perp} = -(2c_{13}/c_{33})\epsilon_{||}$, here c_{13} and c_{33} are the elastic constant known commonly in the literature) are given in Table 2. The lattice parameters were taken as $a = 3.189$ Å and $c = 5.185$ Å for powder GaN and $a = 3.545$ Å and $c = 5.703$ Å for powder InN.[15,16] Parallel and perpendicular strain ratios decrease or increase with increasing SR speed and In content and values are approximately in the order of 10^{-2} and 10^{-3}

for every sample, which shows that the structures are fully strained and there is a weak relaxed layer as seen in Table 2.

The narrowing of FWHM indicates higher quality material. The smallest FWHM values of symmetric (002) reflection peaks belong to sample 128 with different THF and the smallest In content value. It was observed that, depending on SR, when the In content decreases, the FWHM values generally decrease in InGaN layers.

In hexagonal systems, three types of dislocations are observed, screw, edge and mixed; these commonly known defects affect the peak broadening of the reflection $(hkil)$ with $i = -h - k$. They are determined with the equation[17–19]

$$N_{\text{screw}} = \frac{\text{FWHM}^2_{(002)}}{2b^2_{\text{screw}}}, \quad N_{\text{edge}} = \frac{\text{FWHM}^2_{(121)}}{2b^2_{\text{edge}}}. \quad (1)$$

FWHM is measured by HRXRD rocking curves, and b is the Burgers vector length ($b_{\text{screw}} = 0.5185$ nm; $b_{\text{edge}} = 0.3189$ nm for GaN). For InGaN, as the Burgers parameters, one uses the lattice parameters along a and c; they are given in Table 1. As is well known, the tilt range of the lattice planes for wurtzite layers reflects the content of screw TDs with a Burgers vector $b = \pm[001]$, and the twist range of lattice planes reflects the content of edge-type dislocations with a Burgers vector $b = \pm[100]$, $b = \pm[110]$ and $b = \pm[010]$. All defects reflect content of mixing type dislocation ($N_{\text{screw}} + N_{\text{edge}}$) with a Burgers vector $b = \pm[101]$, $b = \pm[011]$ and $b = \pm[111]$. In Fig.2, the calculated dislocation densities are presented as functions of SR. Screw type dislocation shows an

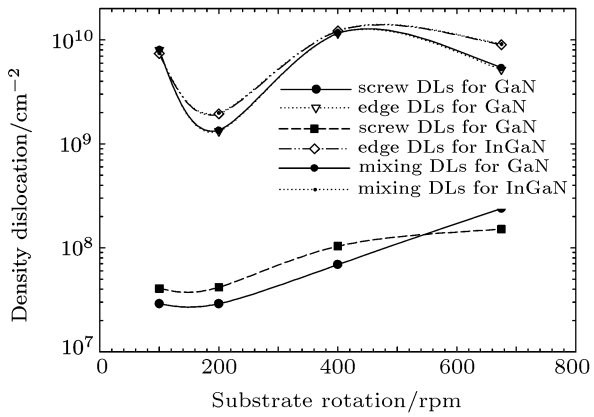


Fig.2. Edge and screw type dislocation versus SR for samples grown in identical conditions.

increasing behaviour but the edge and mixing type dislocations exhibit a waving along increasing SR and they change from $\sim 10^7$ cm^{-2} to 10^{10} cm^{-2}.

In wurtzite hexagonal structures, the defects stay in asymmetric planes more than symmetric planes. These asymmetric planes give better information about quality of the structure. The (102) plane is distorted from all defects and therefore its peak broadening will be called a relative defect. Figure 3 shows relative defects versus SR. In the figure, it shows decreasing and then increasing behaviour with increasing SR. At the same time, this behaviour is valid for a Phi scan (taken by rotating the sample around the (102) asymmetric plane) as shown in Fig.3.

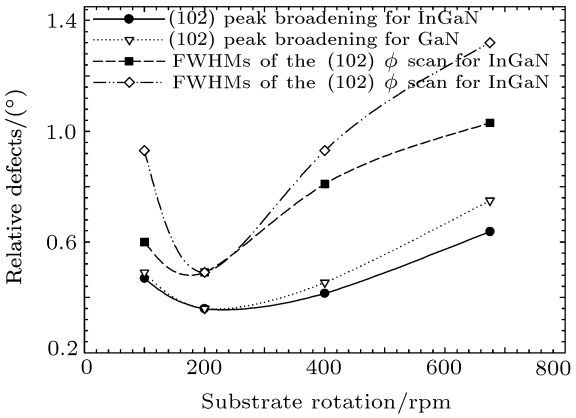


Fig.3. Relative defect versus SR for samples grown in identical conditions.

Electrical resistivity and Hall measurements were performed on each sample in the temperature range of 20–350 K to investigate electrical properties. Hall measurements indicated n-type behaviour, which may be due to the presence of nitrogen vacancies.[20] Since the equilibrium vapour pressure of nitrogen over InN is several orders of magnitude higher than that of GaN, the growth temperature of InGaN is generally lower than that of GaN. The decomposition rate of ammonia (NH_3) becomes low at low growth temperatures, so the high background carrier concentration of undoped InGaN may be ascribed to the nitrogen vacancy increase.[21] Electrical resistivity, Hall mobility and Hall carrier density at room temperature are shown in Table 3: the lowest carrier density is 4.25×10^{18} cm^{-3}, while the highest is 2.85×10^{19} cm^{-3}.

In content versus SR is shown in Fig.4. From Fig.4 a linear relationship between SR (RPM) versus In content is almost observed. This may be explained by an increase of growth rate due to the faster SR speed.[4] Although the In content of sample 128 is not very different from other samples, its resistivity is very small. Also, the carrier density of sample 128 was obtained as 2.85×10^{19} cm^{-3} which is the highest value of all. With this carrier density, sample 128 may be

regarded as a 'metallic' semiconductor system. Therefore sample 128 exhibits metallic behaviour with a resistivity value about $10^{-3}\Omega$·cm.

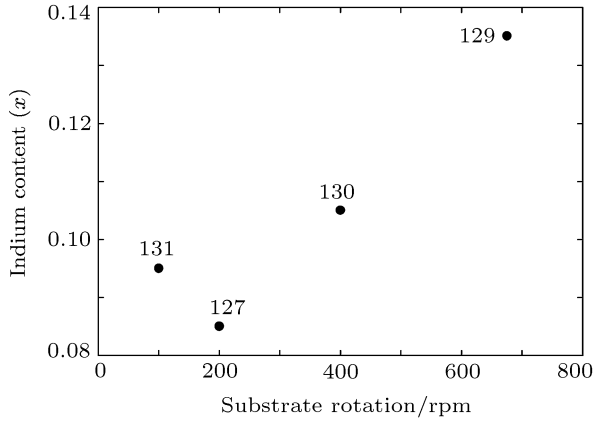


Fig.4. In content versus SR for samples grown in identical conditions.

This different behaviour is observed in the resistivity versus temperature plot. Figure 5 shows a semi log plot of the resistivity versus $1/T$ in the range between 20 and 350 K. Except for sample 128, the resistivity decreases exponentially with increasing temperature for the samples, which is typical semiconductor behaviour. Although samples 127 and 128 were grown with the same SR speed but different THF values, they exhibit different behaviour with temperature as seen in Fig.5. It is interesting that sample 128 has a very slightly temperature dependent resistivity.

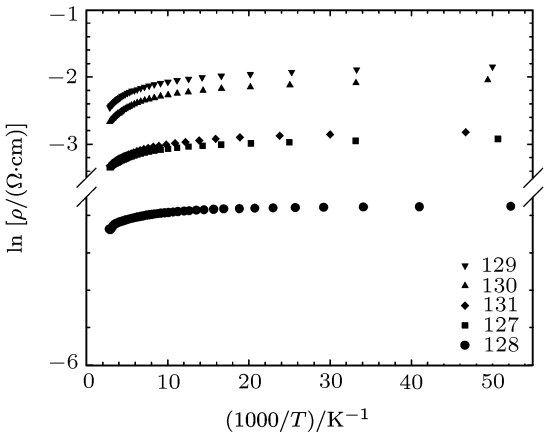


Fig.5. Temperature dependence of resistivity for InGaN alloys.

Activation energies of InGaN alloys were obtained from the plots of log ρ vs $1/T$ for two temperature regions. Apart from sample 128, for the samples the values of activation energies changed from 0.42 to 0.71 meV in the low temperature region $T < 60$ K, while they changed from 10.2 to 15.5 meV in the high temperature region $T > 60$ K. Sample 128 has value of activation energies 0.065 and 2.48 meV for low and high temperature regions respectively. It was observed that all activation energies were smaller than the thermal energy at room temperature (25 meV). The activation energies for resistivity in the low temperature range are smaller than those evaluated from the high temperature range. A very low value of activation energies for the lower temperature region indicates that impurity band conduction may be the dominant transport mechanism in InGaN layers.[20]

Hall mobility is an important parameter to characterize the microscopic quality of semiconductors. The room temperature Hall mobility values are also given in Table 3. From Table 3, it can be seen that mobilities of InGaN alloys are low in comparison to InN or GaN samples in the literature, probably because of alloy scattering, as given by Philip's electronegative difference theory.[22] At room temperature the highest mobility of investigated samples obtained was about 40.6 $\mathrm{cm}^2/(\mathrm{V}\cdot\mathrm{s})$.

Table 3. Room temperature electrical properties of InGaN alloys.

sample	In content x	ρ /(Ω·cm)	μ_{H} /(cm^2/(V·s))	n_{H} /cm^{-3}
#128	0.060	0.0052	40.6	2.85×10^{19}
#131	0.095	0.0379	20.8	7.91×10^{18}
#127	0.085	0.0369	22.5	7.51×10^{18}
#130	0.105	0.0746	15.5	5.44×10^{18}
#129	0.135	0.0917	16.0	4.25×10^{18}

From Table 3, it can be seen that as the indium content increases, the mobility decreases. It can be expected that, as the In mole fraction increases, the effective mass of InGaN alloy decreases, since InN and GaN have $0.115m_0$ and $0.22m_0$ effective (m_0 is the free electron mass) mass values, respectively. Also it is known that InN possesses superior transport properties to GaN over a wide temperature range.[21] Finally, the mobility of $\mathrm{In}_x\mathrm{Ga}_{1-x}\mathrm{N}$ alloys is expected to increase with increasing In content because of the decreased effective mass and increased quantity of InN for $x > 0.4$.[23] However, for the studied InGaN layers, mobility values are still very low in comparison with high quality InGaN layers. This mobility behaviour suggests that the more indium is added to the alloy, the more scattering centres are created, thus lowering carrier mobility for $x < 0.14$.

Figure 6 shows PL spectra taken at room temperature using a He–Cd laser as an excitation source in identical conditions. The main PL peaks are

located between 360 and 640 nm with intensities changing dramatically among different samples; it is valuable to note that in the structure there are several factors contributing to the energy shift, such as In mole fraction, internal stress, piezoelectric field

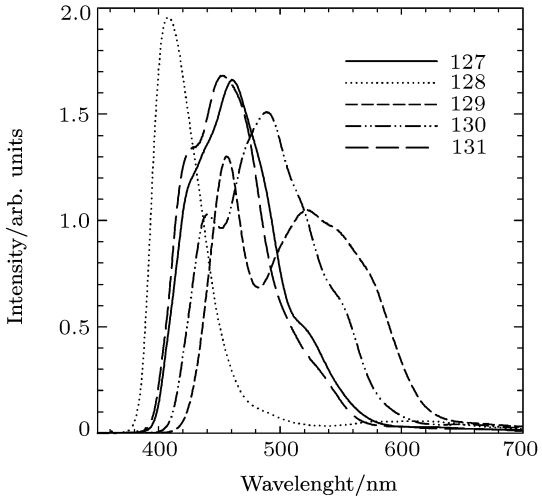


Fig.6. Room-temperature PL spectra for InGaN alloys.

polarization and so on. In our samples, the SR and THF strongly affect the main peak's emission positions of all samples except sample 128. It is concluded that when the SR increases, PL spectra shift regularly along the increasing wavelength. But sample 128 exhibits very high luminescence efficiency and shifts to low wavelengths in a different way with respect to all other samples. The reason for this may come from the higher THF, indicating a strong hydrogen influence in controlling the optical properties of the investigated samples.

4. Conclusion

SR strongly affects the structural, electronic and optical properties of InGaN layers. It was observed that the HRXRD peaks of samples shifted towards lower angles when the SR speed increased. The increase in the SR speed changes other structural properties such as strain, lattice parameter and In content. This case affects the electrical and optical properties. Mosaic structure is not an important change in the defects, and it improves the quality of the crystal structure, especially with SR speed. It was also observed that as THF increases, the main PL peak shifts towards lower wavelength and the electrical resistivity reduces suddenly; it also exhibits metallic behaviour with very slightly dependence on temperature. THF showed more efficiency than SR for the above properties.

References

[1] Huyal O, Ozel T, Koldemir U, Nizamoglu S, Tuncel D and Demir H V 2008 *Optics Express* **16** 1115

[2] Ozel T, Sari E, Nizamoglu S and Demir H V 2007 *J. Appl. Phys.* **102** 113101

[3] Korcak S, Ozturk M K, Corekci S, Akaoglu B, Yu H, Cakmak M, Saglam S, Ozcelik S and Ozbay E 2007 *Surface Science* **601** 3892

[4] Bosi M and Fornari R 2004 *J. Cryst. Growth* **265** 434

[5] Fornari R, Bosi M, Avella M and Martin Jimenez 2002 *J. Semiconducting and Insulating Materials* **12th** International Conference, 30 June–5 July p76

[6] Koukitu A, Taki T, Takahashi N and Seki H 1999 *J. Cryst. Growth* **197** 99

[7] Piner E L, Behbehani M K, ElMasry N A, McIntosh F G, Roberts J C, Boutros K S and Bedair S M 1997 *Appl. Phys. Lett.* **70** 461

[8] Hashımoto M, Amano H, Sawaki N and Akasaki I 1984 *J. Cryst. Growth* **68** 163

[9] Karman Von 1921 *Math. Mech.* **1** 233

[10] Oliver R A, Kappers M J, Humphreys C J, Andrew G and Briggs D 2005 *J. Appl. Phys.* **97** 013707

[11] Williamson G K and Hall W H 1953 *Acta Metall.* **1** 22

[12] Heinke H, Kirchner V, Einfeldt S and Hommel D 1999 *Phys. Stat. Sol.* (a) **176** 391

[13] van de WallChris G, McCluskey M D, Master C P, Romano L T and Johnson N M 1999 *Materials Science and Engineering* B **59** 274

[14] O'Donnell K P, Mosselmans J F W, Martin R W, Pereira S and White M E 2001 *J. Phys.: Condens. Matter* **13** 6977

[15] Balkas C, Basceri C and Davis R 1995 *Powder Diffraction* **10** 266

[16] Paszkowicz W 1999 *Powder Diffraction* **14** 276

[17] Gay R, Hirsch P B and Kelly A 1953 *Acta Metall.* **1** 315

[18] Ide T, Shimizu M, Shen X Q, Jeganathan K, Okumura H and Nemoto T 2002 *J. Cryst. Growth* **245** 15

[19] Heying B, Wu X H, Keller S, Li Y, Kapolnek D, Keller B P, DenBaars S P and Specka J S 1996 *Appl. Phys. Lett.* **68** 29

[20] Roy R K, Gupta S and Pal A K 2005 *Thin Solid Films* **483** 287

[21] Kumakura Kazuhide, Makimoto Toshiki and Kobayashi Naoki 2003 *J. Appl. Phys.* **93** 3370

[22] Farahmand M, Garetto C, Belloti E, Brennan K F, Goano M, Ghilino E, Ghione G, Albrecht J D and Ruden P P 2001 *IEEE Trans. Electron Dev.* **48(3)** 535

[23] Aydogdu S and Ozbas O 2005 *Material Science in Semiconductor Processing* **8** 536